

# Dynamic nuclear polarisation enhanced $^{14}\text{N}$ overtone MAS NMR spectroscopy: Supporting information

Aaron J. Rossini,<sup>a</sup> Lyndon Emsley<sup>a</sup> and Luke A. O'Dell<sup>b\*</sup>,

<sup>a</sup>Centre de RMN à Très Hauts Champs, Institut de Sciences Analytiques, Université de Lyon  
(CNRS/ENS Lyon/UCB Lyon 1), 69100 Villeurbanne, France

<sup>b</sup>Institute for Frontier Materials, Deakin University, Waurn Ponds Campus, Geelong, Victoria 3220,  
Australia

\*Corresponding author: [luke.odell@deakin.edu.au](mailto:luke.odell@deakin.edu.au)

- S1.  $^{14}\text{N}$  NMR parameters used in the simulations
- S2. Glycine  $^{13}\text{C}$  CP DNP enhancement
- S3. Glycine  $^{14}\text{N}^{\text{OT}}$  CP on resonance with  $+2\omega_r$  and  $+\omega_r$  overtone sidebands
- S4. Glycylglycine  $^{13}\text{C}$  CP DNP enhancement
- S5. Simulations modelling the effect of the contact time on the  $^{14}\text{N}^{\text{OT}}$  powder pattern
- S6. Histidine.HCl.H<sub>2</sub>O  $^{13}\text{C}$  CP DNP enhancement
- S7. Quantification of  $^{13}\text{C}$ - $^{14}\text{N}^{\text{OT}}$  HMQC coherence transfer efficiency
- S8. Comparison of  $^{14}\text{N}^{\text{OT}}$  and  $^{15}\text{N}$  sensitivities

## S1. $^{14}\text{N}$ NMR parameters used in the simulations

Sample	Site	$C_Q$ / MHz	$\eta_Q$	$\delta_{\text{iso}} (^{15}\text{N})$ / ppm
Glycine	N1	1.18	0.53	-6
Glycylglycine	N1	1.40	0.10	-12
	N2	3.29	0.45	79
Histidine.HCl.H <sub>2</sub> O	N1	1.25	0.35	8
	N2	1.52	0.25	138
	N3	1.21	0.94	152

Table S1 – NMR parameters used to simulate the  $^{14}\text{N}^{\text{OT}}$  MAS spectra of the various sites for the three samples studied. The isotropic chemical shifts  $\delta_{\text{iso}}$ , which determine the position of the  $^{14}\text{N}^{\text{OT}}$  powder patterns, were measured from the  $^{15}\text{N}$  CPMAS spectra and were fixed in the  $^{14}\text{N}^{\text{OT}}$  simulations. The quadrupolar parameters  $C_Q$  and  $\eta_Q$ , which determine the shape and width of the powder patterns, were adjusted to match the simulated spectra to the experimental  $^{14}\text{N}^{\text{OT}}$  data, using values calculated from density functional theory as initial guesses.

## S2. Glycine $^1\text{H}$ and $^{13}\text{C}$ CP DNP enhancement

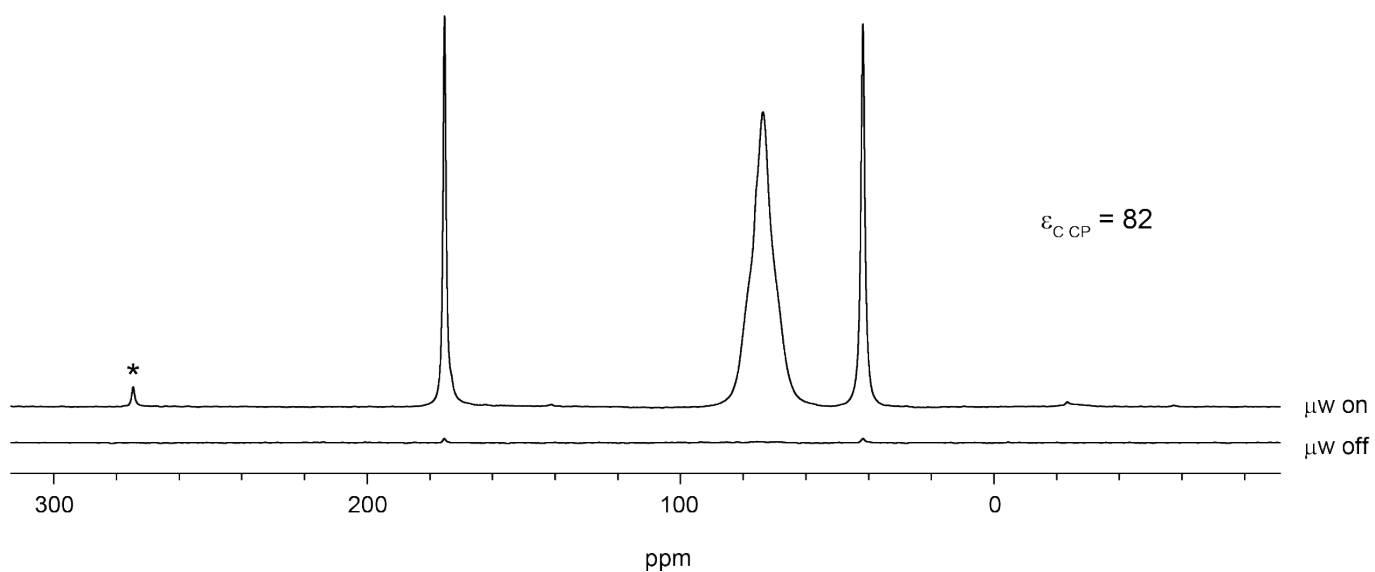


Figure S2  $^{13}\text{C}$  CPMAS NMR spectra obtained from a solid powder sample of glycine impregnated with a solution of TEKPol in tetrachloroethane, with and without 70 mA microwave irradiation applied. The spectra were obtained at 9.4 T, 107 K and 10 kHz MAS (4 scans with 10 s recycle delay and 2 ms cross-polarisation contact time). Asterisks denote spinning sidebands. The  $^{13}\text{C}$  signal from the TCE is visible at 74 ppm.

### S3. Glycine $^{14}\text{N}^{\text{OT}}$ CP on resonance with $+2\omega_r$ and $+\omega_r$ overtone sidebands

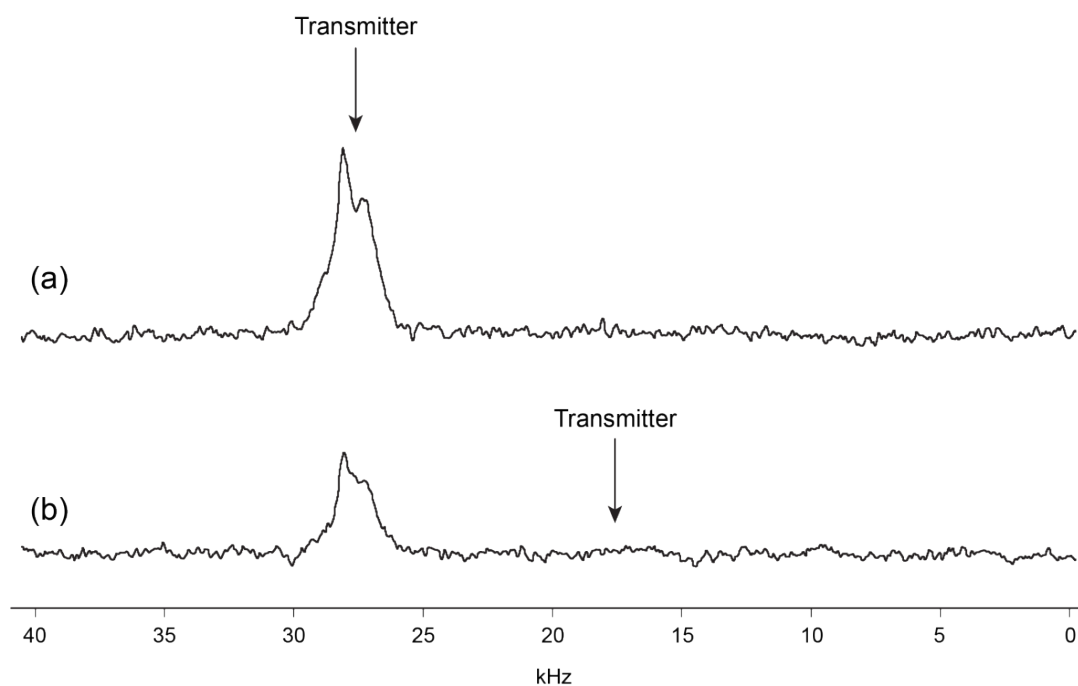


Figure S3 – DNP-enhanced  $^{14}\text{N}^{\text{OT}}$  CPMAS spectra obtained from a solid powder sample of glycine impregnated with a solution of TEKPol in tetrachloroethane, at 9.4 T and 107 K. Both spectra were obtained at 10 kHz MAS with a CP contact time of 125  $\mu\text{s}$ , 16 scans and a recycle delay of 40 s. In spectrum (a) the  $^{14}\text{N}^{\text{OT}}$  transmitter frequency was placed on resonance with the  $+2\omega_r$  overtone sideband as shown. In (b) this frequency was adjusted by  $-10$  kHz, but no  $+\omega_r$  overtone sideband was observed.

#### S4. Glycylglycine $^{13}\text{C}$ CP DNP enhancement

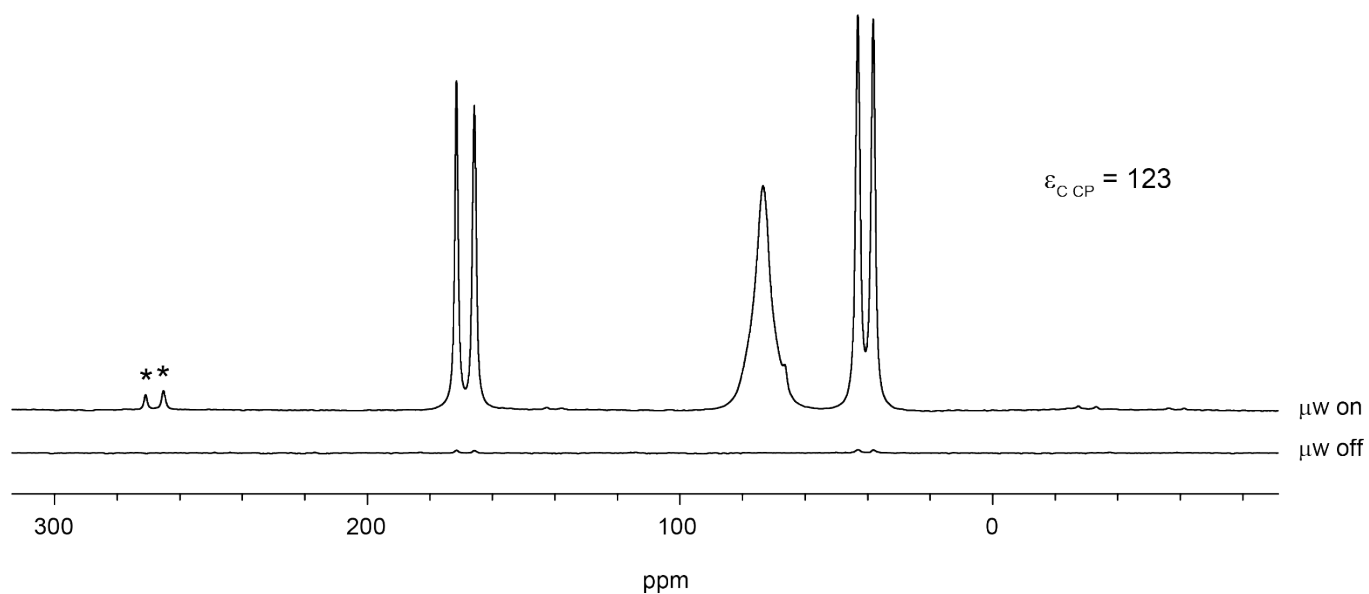


Figure S4 –  $^{13}\text{C}$  CPMAS NMR spectra obtained from a solid powder sample of glycylglycine impregnated with a solution of TEKPol in tetrachloroethane, with and without 70 mA microwave irradiation applied. The spectra were obtained at 9.4 T, 107 K and 10 kHz MAS (4 scans with 10 s recycle delay and 2 ms cross-polarisation contact time for  $^{13}\text{C}$ ). Asterisks denote spinning sidebands, and the  $^{13}\text{C}$  signal from the TCE is visible in at 74 ppm.

## S5. Simulations modelling the effect of the contact time on the $^{14}\text{N}^{\text{OT}}$ powder pattern

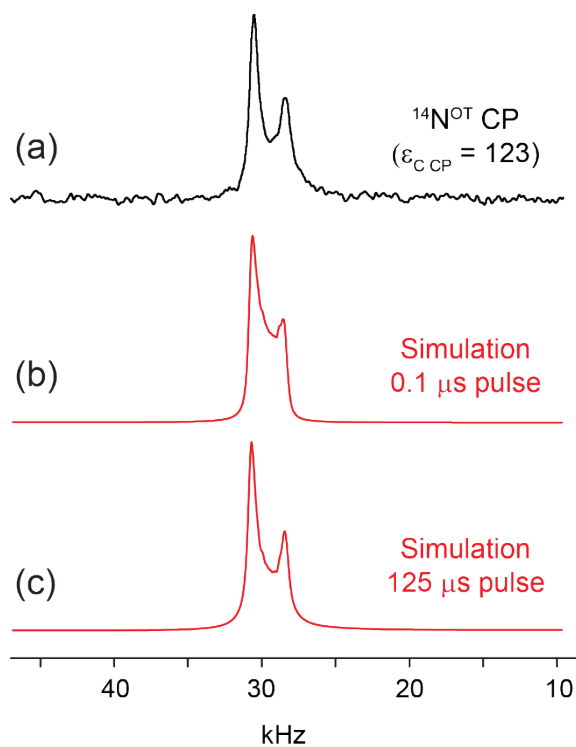


Figure S5 – (a)  $^{14}\text{N}^{\text{OT}}$  spectrum obtained from glycyglycine at 107 K, 9.4 T and 10 kHz MAS using DNP-enhanced cross-polarisation from the  $^1\text{H}$  nuclei, with a CP contact time of 125  $\mu\text{s}$  and the  $^{14}\text{N}^{\text{OT}}$  contact pulse applied on resonance with the N1 peak at 30 kHz. 20 scans were acquired with a recycle delay of 40 s. Simulations made using pulse lengths of (b) 0.1  $\mu\text{s}$  and (c) 125  $\mu\text{s}$  are also shown to model the effects of the contact time on the powder pattern shape.

## S6. Histidine.HCl.H<sub>2</sub>O <sup>13</sup>C CP DNP enhancement

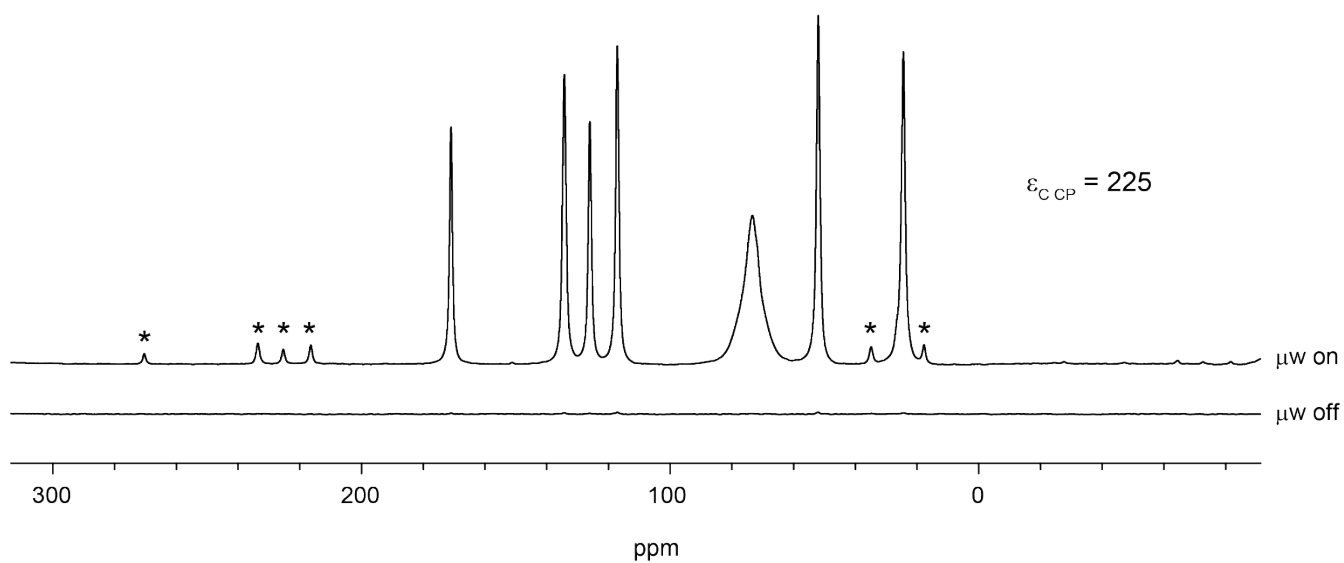


Figure S6 – <sup>13</sup>C CPMAS NMR spectra obtained from a solid powder sample of histidine.HCl.H<sub>2</sub>O impregnated with a solution of TEKPol in tetrachloroethane, with and without 70 mA microwave irradiation applied. The spectra were obtained at 9.4 T, 107 K and 10 kHz MAS (4 scans with 10 s recycle delay and 2 ms cross-polarisation contact time for <sup>13</sup>C). Asterisks denote spinning sidebands, and the <sup>13</sup>C signal from the TCE is visible in at 74 ppm.

## S7. Efficiency of $^{13}\text{C}$ - $^{14}\text{N}^{\text{OT}}$ HMQC filters

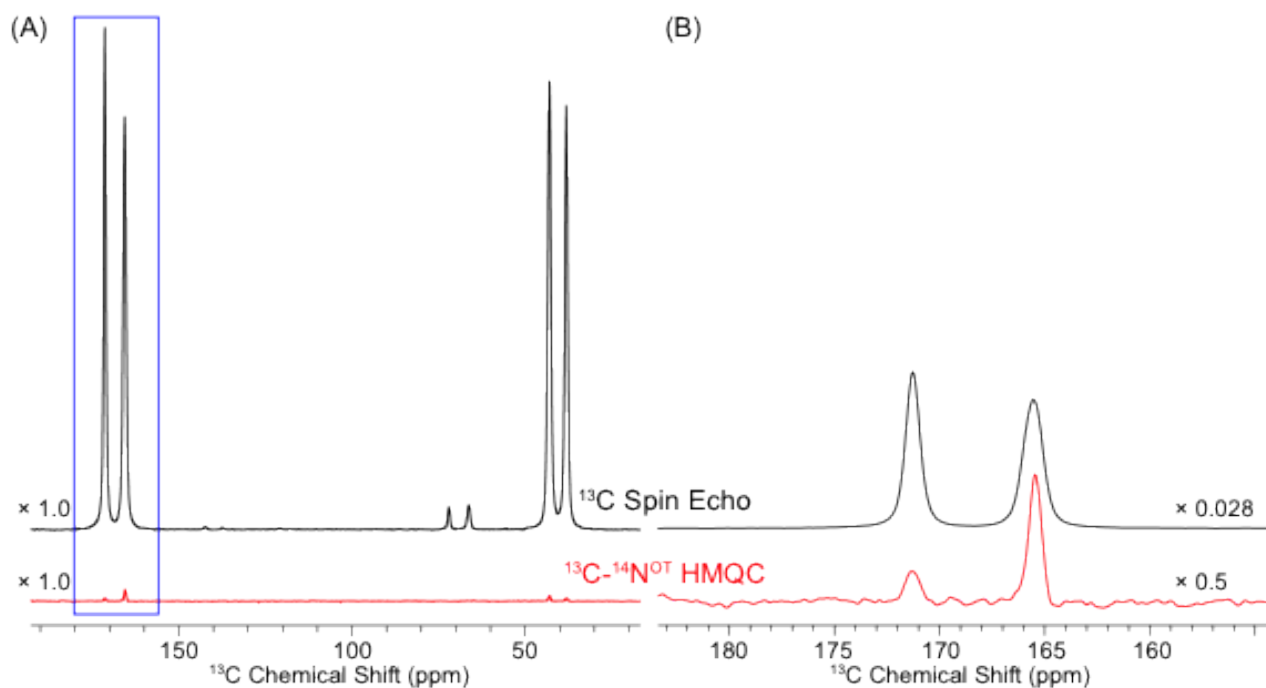


Figure S7 – Comparison of DNP enhanced  $^1\text{H}$ - $^{13}\text{C}$  CP spin echo spectrum (16 scans) and  $^1\text{H}$ - $^{13}\text{C}$  CP HMQC  $^{14}\text{N}^{\text{OT}}$  filtered spectrum (32 scans) acquired with a  $200\ \mu\text{s}$   $^{14}\text{N}^{\text{OT}}$   $90^\circ$  pulse applied on resonance with the amide (-NH) nitrogen for coherence transfer. In both cases the total  $^{13}\text{C}$  transverse magnetization evolution time was 15 ms. The efficiency of the  $^{14}\text{N}^{\text{OT}}$  HMQC filter is 2.8%. In both cases a 10 s recycle delay was employed.



## S8. Comparison of $^{14}\text{N}^{\text{OT}}$ and $^{15}\text{N}$ sensitivities

Sample	Site	Number of scans		Experiment time / min		Line width / Hz		S/N		$\epsilon_{\text{C CP}}$	
		$^{14}\text{N}^{\text{OT}}$	$^{15}\text{N}$	$^{14}\text{N}^{\text{OT}}$	$^{15}\text{N}$	$^{14}\text{N}^{\text{OT}}$	$^{15}\text{N}$	$^{14}\text{N}^{\text{OT}}$	$^{15}\text{N}$	$^{14}\text{N}^{\text{OT}}$	$^{15}\text{N}$
Glycine	N1	16	8	11	8	1500	34	34	291	82	80
Glycylglycine	N1	32	8	32	8	3000	36	33	140	123	84
	N2	32		32		8500	34	13	153		
Histidine.HCl.H <sub>2</sub> O	N1					2000	35	19	78		
	N2	64	8	64	8	4000	28	15	98	225	72
	N3					1500	50	25	60		

Table S2 – Comparison of factors contributing to  $^{14}\text{N}^{\text{OT}}$  and  $^{15}\text{N}$  sensitivities in the directly-observed, DNP-enhanced spectra acquired in this work. Other experimental details can be found in the main article. All spectra were acquired at 9.4 T and a temperature of around 107 K.